Materials Advances

ROYAL SOCIETY OF CHEMISTRY

PAPER

Check for updates

Inverse vulcanization of octenyl succinate-modified corn starch as a route to biopolymer–sulfur composites†

Moira K. Lauer,[a] Andrew G. Tennyson [ID] [ab] and Rhett C. Smith [ID] *[a]

Herein we report a route to sulfur–starch composites by the modification of corn starch with octenyl succinic anhydride (**OSA**, degree of substitution = 2.6%) and its subsequent reaction with elemental sulfur through an inverse vulcanization process to generate **OSSx** (where x = wt% sulfur, either 90 or 95). This work represents an expansion into a previously untapped biomass source for the preparation of recyclable thermoplastic materials by this process. Composites **OSSx** are comprized of 83–89% by mass of extractable sulfur, and have reasonable thermal stability (T_d = 214–216 °C) and T_m (DSC) of 118 °C. The starch modification strategy employed herein allowed for lower degree of substitution of the starch than was feasible for other biploymers, leading to materials with high strength despite relatively low crosslink density relative to that in previous biopolymer–sulfur composites. The low crosslink density resulted in relatively long polysulfur catenates, thus producing materials with impressive flexural strengths (5.3–5.4 MPa) and highlighting the potential for biomass–sulfur materials to exhibit a range of mechanical properties depending on the biopolymer scaffold and modification strategy.

Introduction

Inverse vulcanization has recently gained attention as a way to valorise waste sulfur from petroleum refining by its reaction with a wide range of substrates to give high sulfur-content materials (HSMs).[1,2] Inverse vulcanization is a process involving reaction of a majority feed ratio of sulfur with an olefin-bearing comonomer. Theoretically this process can be up to 100% atom economical, as mechanistically inverse vulcanization proceeds *via* the radical pathway shown in Scheme 1. Through this process materials have been developed for a multitude of applications including IR transparent lenses, cathodes for lithium–sulfur batteries, and materials for oil spill remediation and mercury capture.[4–20] More recently, novel strategies have been implemented for inverse vulcanization at reduced temperatures as well as for processing/recycling[23–26] HSMs prepared by inverse vulcanization.[27–31] Similar HSMs can be prepared from the reaction of aryl halides or anisole derivatives with sulfur as well, although polymerization of these monomers proceeds *via* different mechanisms than simple inverse vulcanization.[32–35]

In addition to the aforementioned applications of HSMs, our group has recently reported numerous high-strength composite materials prepared by the reaction of sulfur with bio-derived monomers including fatty acids,[36–39] triglycerides,[42] terpenoids,[21,43] amino acid derivatives,[44] lignin derivatives,[22,35,45,46] cellulose derivatives,[3,21] and raw lignocellulosic biomass sources.[40,41] In terms of commercialization of biopolymer-derived materials, starch-derived films and composites have recently gained tremendous interest because starch is remarkably simple to solubilize, derivatize and process compared to cellulose. We recently reported a comprehensive review on the merits and progress in application of starch as a structural element for packaging applications.[47] Given the desirable properties of starch and its chemical similarity to cellulose, we hypothesized that starch may be an attractive target as a comonomer with sulfur in the quest to expand the repertoire of material properties and sustainably-sourced polymers/composites that can be conveniently prepared. We further hypothesized that the desirable processability and sulfur-miscibility of starch would allow durable composites to be prepared from starch requiring a lower degree of substitution than is required

[a] Department of Chemistry, Clemson University, Clemson, South Carolina, 29634, USA. E-mail: rhett@clemson.edu

[b] Department of Materials Science and Engineering, Clemson University, Clemson, South Carolina, 29634, USA

† Electronic supplementary information (ESI) available: Proton NMR spectral data, FTIR spectra, TGA curves, analysis of char yield *versus* composition; DSC curves. See DOI: 10.1039/d0ma00948b
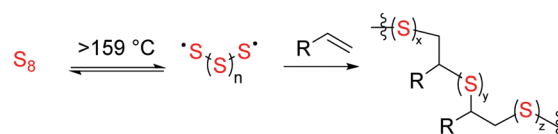
Scheme 1 Simplified schematic for the inverse vulcanization process.

when cellulose is employed as the biopolymer element, thus limiting the amount of non-bio-derived material in the composites.

Starch is ubiquitous and easily produced worldwide, making it a resilient candidate for exploration as a component of sustainable surrogates for environmentally deleterious polymers that plague society. Corn starch is of particular interest as corn is one of the most-produced crops globally and corn starch is typified by smaller and more uniform particle sizes relative to other starch sources.[48,49] In 2020, more than 15 billion bushels of corn were produced in the U.S. alone, approximately 70% of which is comprised of starch.[47,50] In 2015, approximately 50% of all corn was utilized for animal feed, 30% for bioethanol production, 6% to produce sweeteners, and 11% for export.[51] Current trends in food consumption and the demand for more health-conscious options have led to commensurate decrease in the demand for corn-based sweeteners and an increase in the demand for grass-fed, rather than grain-fed cattle.[52,53] These trends, coupled with a nearly 50% reduction in the price of corn since 2013 yet constant production volume (Fig. 1) posture corn starch as an untapped potential resource in the development of more value-added and sustainable technologies.

In the current study, we have thus modified commercial corn starch with octenylsuccinic anhydride (**OSA**) in order to equip starch with the olefins required for reaction with sulfur through inverse vulcanization. The thermal and mechanical properties of the resultant composites (**OSSx**, where x = wt% sulfur, either 90 or 95 wt%, Scheme 2) were analysed for comparison to analogous properties of other biomass–sulfur composites.

Results and discussion

Starch modification and composite synthesis

Modification of corn starch was carried out by its reaction with octenylsuccinic anhydride (**OSA**) *via* a standard literature procedure.[54] This particular modification protocol was selected for its favourable incorporation of green chemistry principles: the reaction is carried out at room temperature in aqueous media (full details can be found in the ESI†), to yield **OSA**-modified starch **OS** (Scheme 2). Olefination with **OSA** is also well-precedented to give a product with limited change in
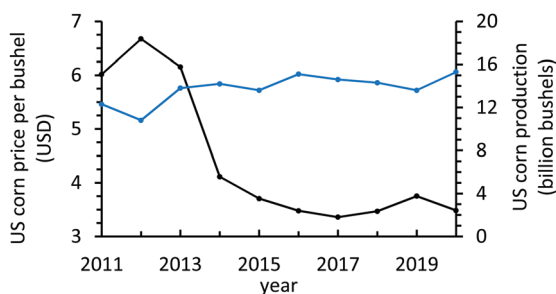

Fig. 1 Trends in the yearly average corn price per bushel (black) and the yearly U.S. corn production (blue) showing relatively steady production but a significant drop in price due to reduced consumer demand.

crystallinity upon functionalization.[55] In our previous work, we have noted that retention of biopolymer crystallinity is a potential contributing factor in compatibilizing sulfur and biopolymer comonomers as well as for imbuing strength to the resultant cellulose–sulfur composites.[3,21] The incorporation of hydrophobic alkyl chains should also improve miscibility/ compatibilization with sulfur for more facile reaction than has been observed in some cellulose–sulfur systems.[56] Modification with **OSA** also provides another site for modification, a carboxylic acid side chain, which could be further functionalized to incorporate additional olefins to increase crosslink density, although this avenue is not described in the current work.

Successful modification of the corn starch was qualitatively confirmed by ATR-FTIR spectroscopic analysis, which revealed carbonyl stretches at 1566 and 1639 cm^{-1} attributable to ester and carboxylic acid functionalities, while the C–H stretching of the olefin functionality was too weak to observe (ESI,† Fig. S1). The degree of substitution (DS, the number of olefins per anhydroglucose unit) in **OS** was determined to be 0.0263 ± 0.0005 by acid–base titration. Modification of starch with **OSA** resulted in a drastic change in hydrophilicity, a property that was readily visualized by qualitative observation of the significantly higher contact angle with water for **OS** than for native corn starch (Fig. 2A). This observation is consistent with reported quantitative studies that demonstrate significant increases in water contact angle with **OSA**-modified starch films having DS < 0.03.[57]

The thermal properties of **OS** were also noticeably different from those of native corn starch. The decomposition temperature (T_d) as assessed by thermogravimetric analysis (TGA) decreased by approximately 25 °C upon modification (293.5 ± 0.5 for **OS** *versus* 268.4 ± 0.4 °C for corn starch; Table 1 and ESI,† Fig. S2 and Table S1). The glass transition temperature (T_g) determined from differential scanning calorimetry (DSC) decreased by approximately 9 °C upon modification (98.4 and 89.6 °C for corn starch and **OS**, respectively, ESI,† Fig. S3). As anticipated, the crystallinity showed a decreased of only 5%, from 20.9% for native corn starch to 15.8% for **OS**, as determined by powder X-ray diffraction (PXRD, ESI,† Fig. S4).

Synthesis of **OS**–sulfur composites (**OSSx**, where x = wt% sulfur, either 90 or 95 wt%, Scheme 2) was undertaken under an inert atmosphere of N$_2$ at 180 °C. In this process, each of the modified monomers provided one olefin for potential reaction *via* inverse vulcanization (Scheme 1). Although **OS** was significantly more miscible with sulfur than native corn starch, the homogenization of **OS** granules with sulfur still proved challenging and required constant efficient stirring due to phase separation at the reaction interface. Unsurprisingly, homogenization with a higher ratio of **OS** (*i.e.* **OSS**$_{90}$) required longer reaction times. To eliminate any heating-duration effects, however, both samples were heated for 440 minutes at 180 °C, the conditions required to homogenize the **OSS**$_{90}$ reaction mixture. The resultant materials were allowed to cool before remelting and pouring into appropriate moulds to shape the material into rectangular prisms or cylinders for flexural and compressional strength analysis, respectively. Both materials were golden-brown in colour upon cooling, with **OSS**$_{95}$ taking on a slightly darker colour (Fig. 2B). All subsequent thermal,
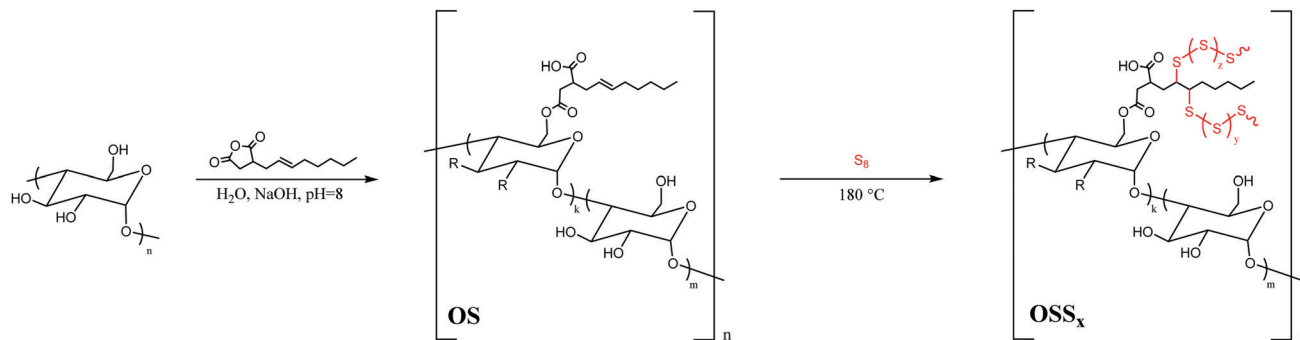
Scheme 2 The reaction of starch, shown as poly((1 → 4)α-D-glucopyranose) for simplicity, with octenylsuccinic anhydride (**OSA**) to yield **OS** where $k = 0.0263$ and $m = 0.9737$ and the subsequent reaction of olefinic **OS** with sulfur which can occur above 159 °C when cyclic S_8 homologates to form radical polymeric sulfur to generate **OSS**x, (where x = wt% sulfur, either 90 or 95 wt%).
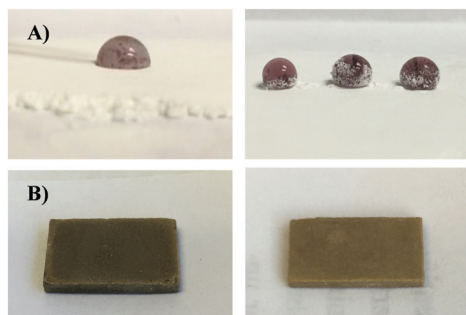

Fig. 2 (A) The increase in water contact angle from an unmodified corn starch film (left, after 0.1 s exposure; eventually water is absorbed by starch) to an **OS** film (right) provides a visual, qualitative demonstration of increased hydrophobicity upon modification. The water was dyed with food coloring to improve image quality and had no effect on the inter-action between starch and water. (B) Digital images of cuboids of **OSS**$_{95}$ (left) and **OSS**$_{90}$ (right) measuring approximately 15 × 8 × 1.5 mm.

Table 1 Thermal properties of prepared composites and feed materials. Data reported with standard deviations from 3–5 duplicate trials

	$T_d{}^a$ (°C)	Cold xtl.^{b} (°C)	$T_m{}^{cd}$ (°C)	S_8 melt integration^e (J g^{-1})	Char yield^f (%)
Sulfur^c	219.0 ± 2.4^g	—	119	−45.4 ± 1.3	−0.2 ± 0.3
OSS$_{95}$	215.6 ± 0.8	22.6	118	−40.2 ± 1.1	0.6 ± 0.0
OSS$_{90}$	213.8 ± 0.2	24.6	118	−37.5 ± 1.2	1.6 ± 0.3
OS^d	268.4 ± 0.4	—	—	—	11.6 ± 0.1^h

^{a} The average temperature at which 5% mass loss was observed. ^{b} Taken from the third heating cycle. ^{c} Defined as the midpoint of the step in the heat of the DSC thermogram. ^{d} The melting temperature for S_8 determined by the DSC thermogram. ^{e} Taken as an average of the values from heats 3–5 by triplicate analyses. ^{f} Residual mass at 800 °C. ^{g} Values based on quadruplicate analysis due to the poor thermal conductivity of sulfur and the large dependence on the sample mass (varied from 5–6.5 mg across four trials). ^{h} Normalized to eliminate the impact of adsorbed water.

compositional, and mechanical analyses were conducted after samples were cured for 15 days at room temperature to ensure that any metastable polymeric sulfur that was not sufficiently

stabilized by the crosslinked network would relax to the stable S_8 allotrope. The mechanical properties of HSMs can vary wildly within the first few days of their preparation, so this pre-characterization curing is essential if the data are to be used to draw conclusions relevant to eventual practical applications.

Elemental analysis confirmed that **OSS**$_{95}$ and **OSS**$_{90}$ contained 95 and 90 wt% of sulfur, respectively. Although IR spectroscopy was not sensitive enough to assess the consumption of olefins, indirect evidence for successful sulfur crosslinking was abundant. Fractionation of the composites in CS_2 revealed that only 82 and 86% of **OSS**$_{90}$ and **OSS**$_{95}$, respectively, were comprised of CS_2-soluble S_8, indicating that a surprisingly large proportion of sulfur – 8.4 and 10 wt% of monomer feed sulfur for **OSS**$_{95}$ and **OSS**$_{90}$ respectively – was crosslinked. These crosslinkable sulfur values compare to only up to 7.4 wt% of monomer feed sulfur that were stabilized as crosslinking catenates in analogous cellulose–sulfur composites (**PCS**$_x$) despite the fact that there were only ∼20% the available crosslinkable sites in **OSS**x composites (Table 2) compared to the number available in **PCS**x.[58] Sulfur ranks (R_S, average number of sulfur atoms per crosslinking polysulfur chain) were calculated to be 170 and 69 for **OSS**$_{95}$ and **OSS**$_{90}$, respectively (calculations and raw data provided in the ESI† and accompanying Table S2 and eqn (S2)). The R_S in **OSS**x composites are towards the high end of the range reported for previously-reported biopolymer–sulfur composites prepared by inverse vulcanization of methylpropene-derivatized cellulose (**PCS**x, R_S = 24–58),[58] geraniol-derivatized cellulose (**GCS**$_{90}$, R_S = 22),[59] allyl lignin (**LS**x, R_S = 49–96),[46] or allylated lignocellulose biomass (**APS**x, R_S = 20–21).[40,41] A comparison of several properties for **OSS**x and these related biopolymer–sulfur composites is provided in Table 2.

Thermal analysis provides an additional method to quantify the amount of free S_8 *versus* polysulfur catenates in the composite by comparing the integration of the S_8 melt peak in the DSC analysis (Table 1) for pure sulfur and the composites. This analysis revealed that **OSS**$_{90}$ and **OSS**$_{95}$ are comprised by 82.7 ± 4.8% and 89 ± 4.8% S_8, respectively, consistent with the results obtained from CS_2 fractionation. The appearance of a cold crystallization peak in the DSC traces for both materials was also consistent with the presence of a network structure in which crystallization of sulfur is delayed

Table 2 Morphological and mechanical properties of **OSSx** and other biopolymer–sulfur composites for comparison

	Crosslinkable sites[a] (µmol olefin per g composite)	CS$_2$ soluble[b] (%)	Sulfur rank[c]	Flexural strength (MPa)	Flexural modulus (MPa)	Compressional strength (MPa)
OSS$_{95}$	7.84	86	170	5.4	690	11.9 ± 3.2
OSS$_{90}$	15.7	82	69	5.3	660	10.9 ± 1.9
PCS$_{95}$[e]	35.6	88	58	ND[d]	ND[d]	ND[d]
PCS$_{90}$[e]	71.2	84	24	ND[d]	ND[d]	ND[d]
GCS$_{90}$[f]	141	71	22	>4.9	950	ND[d]
LS$_{95}$[g]	45	87	49	ND	ND	ND[d]
LS$_{90}$[g]	73.5	84	96	1.7	60	ND[d]
APS$_{95}$[h]	95.0	89	20	4.8	690	35.7 ± 1.8
APS$_{90}$[h]	190	77	21	6.7	1490	24.1 ± 5.7

[a] Determined by the extent of modification and incorporation of organic material into the composite. [b] The wt% of material that was soluble in CS$_2$ upon fractionation. [c] The average number of sulfur atoms per crosslink. [d] No data were reported in the associated manuscript. [e] Data from the ref. 3. [f] Data from the reference. [g] Data from the ref. 21 and 22 [h] Data from the ref. 40 and 41

due to limited mobility resulting from long polymeric chains.[46,60] The more confined matrix of **OSS$_{90}$** is apparent from the broader cold crystallization peak as well as a later crystallization exotherm on cooling compared to **OSS$_{95}$** (Fig. 3 and Table 1). Thermogravimetric analysis (TGA) revealed only a slight decrease in decomposition temperature (<10 °C) for **OSSx** materials relative to sulfur and char yields consistent with the amount of organic (5 or 10%) present in the materials (ESI,† Fig. S5).

Mechanical properties of biomass–sulfur composites

Some biopolymer–sulfur composites have shown flexural and compressive strengths that exceed those of familiar building materials such as Portland cement (Table 2). The mechanical properties of **OSSx** were measured to assess whether the starch composites could likewise serve as structural materials with lower degrees of olefin substitution than were required in previous biopolymer–sulfur composites. Flexural analysis in a dynamic mechanical analyser revealed that **OSSx** composites possessed strengths on par with other biopolymer–sulfur composites despite the lower crosslink densities (Table 2 and Fig. 4A). Compared to one another, **OSS$_{95}$** and **OSS$_{90}$** behaved almost identically within the regime of recoverable deformation. At higher stresses, however, **OSS$_{90}$** retained much of its rigidity whereas **OSS$_{95}$** deformed significantly, resulting in a

near 40% greater toughness for **OSS$_{95}$** relative to **OSS$_{90}$** (Table 3).

Although the flexural strengths were quite impressive considering the limited crosslinkable sites, this phenomenon did not extend to the compressional strength characteristics. The compressive strengths of **OSSx** (10.9 and 11.9 MPa for **OSS$_{95}$** and **OSS$_{90}$**, respectively) are reasonably strong considering that the compressive strength requirement of Portland cement is ≥17 MPa for residential building, but are less than half the
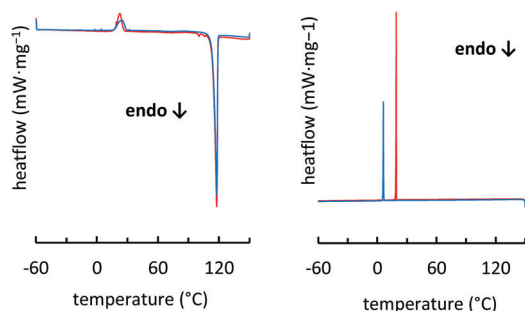

Fig. 3 Sample mass-normalized DSC traces for heating (left) and cooling (right) curves of **OSS$_{95}$** (red) and **OSS$_{90}$** (blue) for the third cycle. **OSS$_{90}$** exhibits a broader cold crystallization exotherm and a reduced sulfur melt peak on heating and a later crystallization exotherm on cooling compared to **OSS$_{95}$**.
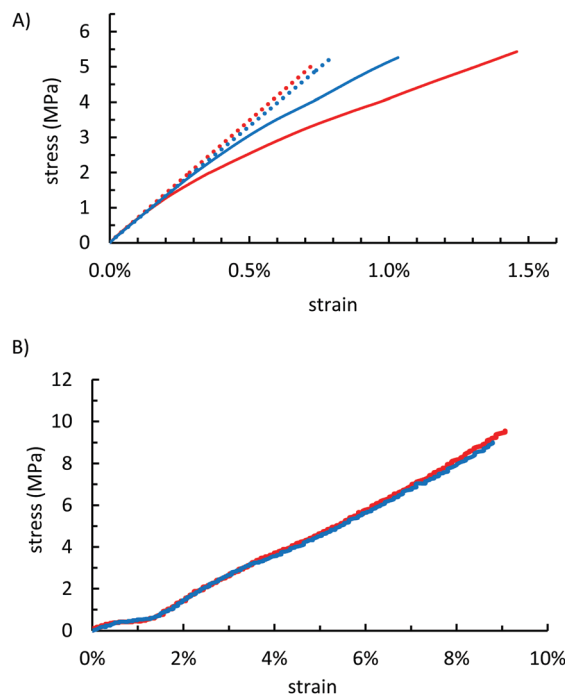

Fig. 4 (A) Flexural stress–strain curves (solid lines) for **OSS$_{95}$** (red) and **OSS$_{90}$** (blue). Although the materials are similarly stiff under a recoverable deformation (linear region denoted by dotted lines), past the proportional limit **OSS$_{90}$** retains much of its rigidity due to a higher crosslink density whereas **OSS$_{95}$** deforms considerably resulting in toughness's of 42.9 and 30.2 kPa for **OSS$_{95}$** and **OSS$_{90}$**, respectively although the materials exhibit similar flexural strengths. (B) Representative compressional stress–strain plots of **OSS$_{95}$** (red) and **OSS$_{90}$** (blue) showing nearly identical responses to compressive stresses.

Table 3 Mechanical parameters determined by flexural stress–strain analysis

	OSS$_{95}$	OSS$_{90}$
Linear strain[a] (%)	0.13	0.31
Linear stress[b] (MPa)	0.9	2.0
Flexural strength (MPa)	5.4	5.3
Flexural modulus (MPa)	690	660
Modulus of resilience[c] (kPa)	0.6	3.2
Max strain[d] (%)	1.46%	1.03%
Toughness[e] (kPa)	42.9	30.2

[a] The deformation at the linear limit as defined by a 0.05 MPa deviation from linearity. [b] The stress at the linear limit as defined by a 0.05 MPa deviation from linearity. [c] The integration at the linear limit. [d] The deformation at sample failure. [e] The integration at sample failure.

values reported for lignocellulose–sulfur composites **APS**$_x$ that were prepared by the inverse vulcanization of allylated peanut shells. Interestingly, **OSS**$_{90}$ and **OSS**$_{95}$ had nearly identical strengths and behaviour under a compressional stress (Table 2 and Fig. 4B) when compared to one another.

Conclusions

Herein is delineated a mechanism for the valorisation of waste sulfur with corn starch. Starch was first modified to a low degree of substitution by reaction with **OSA** at room temperature in aqueous solution. Modified starch was then reacted *via* inverse vulcanization with sulfur to yield biomass–sulfur composites, **OSS***x*. The limited concentration of olefin functionalities present in the modified starch were able to stabilize a surprisingly large amount of polymeric sulfur through crosslinking reactions, resulting in flexural strengths on par or better than previously-prepared biomass–sulfur composites that required more modification for their preparation. Both starch composites had similar strength and flexural behaviour under a recoverable deformation, but the addition of increased organic content resulted in a sustained stiffness with increasing applied force, ultimately reducing its toughness and potentially indicating a finite improvement in mechanical properties by increasing the ratio of organic content. Although the limited degree of crosslinking relative to previously modified biopolymers did not negatively impact flexural properties, it did have a more pronounced attenuation of compressional strength with both materials having nearly identical strengths and behaviour under a compressional deformation. Although this work confirms that starch–sulfur composite materials have potential to be used as structural materials even with their limited degrees of crosslinking, more affordable and sustainable derivatizing agents need to be explored before these types of materials become practically applicable components of sustainable building practices. The long-term stability of high sulfur-content materials is also an open question that must be addressed. Such studies are currently underway to further develop these and related materials for practical applications.

Experimental

General considerations

Fourier transform infrared spectra were obtained using an IR instrument (Shimadzu IRAffinity-1S) with an ATR attachment. Scans were collected over the range 400–4000 cm^{-1} at ambient temperature with a resolution of 8. TGA was recorded (Mettler Toledo TGA 2 STARe System) over the range 20–800 °C with a heating rate of 10 °C min^{-1} under a flow of N$_2$ (100 mL min^{-1}). Each measurement was acquired in duplicate and presented results represent an average value. DSC was acquired (Mettler Toledo DSC 3 STARe System) over the range −60 to 150 °C with a heating rate of 5 °C min^{-1} under a flow of N$_2$ (200 mL min^{-1}). Each DSC measurement was carried out over five heat–cool cycles. Each measurement was acquired in triplicate to ensure consistent results were obtained.

DMA was performed (Mettler Toledo DMA 1 STARe System) in single cantilever mode. DMA samples were cast from silicone resin moulds (Smooth-On Oomoo® 30 tin-cure). Samples were manually sanded to ensure uniform dimensions of approximately 15 × 8 × 1.5 mm but due to instrumental limitations (maximum force of 10 N), each sample differed slightly in thickness in order to obtain a stress at break. Sample dimensions were measured with a digital calliper with ±0.01 mm resolution. Clamping was done by hand due to the samples' brittleness. The force was varied from 0 to 10 N with a ramp rate of 0.2 N min^{-1} measured isothermally at 25 °C.

Carbon disulfide extractions were performed by suspending 0.3 g of finely ground material (measured to 0.0001 g) in 20 mL of CS$_2$, allowing the solid to settle for 30 minutes, pipetting off the supernatant into a separate vial, and adding another 20 mL of CS$_2$. This process was repeated an additional 3 times so that a total of 5 washes was performed. The residual CS$_2$ was evaporated under a flow of N$_2$ and each vial was weighed to determine the fraction that was soluble (collected as supernatant) or insoluble (remained in the initial vial).

Compressional analysis was performed on a Mark-10 ES30 test stand equipped with a M3-200 force gauge (1 kN maximum force with ±1 N resolution) with an applied force rate of 3–4 N s^{-1}. Compression cylinders were cast from silicone resin moulds (Smooth-On Oomoo® 30 tin-cure) with diameters of approximately 6 mm and heights of approximately 10 mm. Samples were manually sanded to ensure uniform dimensions and measured with a digital calliper with ±0.01 mm resolution. Compressional analysis was performed in triplicate and results were averaged.

Powder X-ray diffraction samples were placed on zero background sample holders and analysed using a Rigaku Ultima IV diffractometer with Cu Kα radiation (λ = 1.5406 Å). Data were collected from 5–65 degrees in 2-theta at a rate of 0.5 degree per minute with a sampling interval of 0.02 degrees. Crystallinity calculations were conducted by analysing the data from 5–30 degrees (crystalline peaks at ∼12, 15, 17, 18, 23, and 27 degrees and amorphous peaks at ∼19 and 27 degrees).[61]

Materials and methods

Corn starch (Sigma Aldrich) elemental sulfur (99.5%, Alfa Aesar), octenyl succinic anhydride (97%, mixture of cis and

trans, Sigma Aldrich), sodium hydroxide ($\geq$97% VWR Chemicals), hydrochloric acid (concentrated, VWR), potassium hydrogen phthalate (Aldrich Chemical Company), isopropyl alcohol ($\geq$99.5%, Honeywell), and phenolphthalein (ACS grade, VWR) were all used as received unless otherwise specified.

Details on the synthesis as well as characterization of **OS** can be found in the ESI† (pages, figures, *etc.*).

General composite synthesis

A quantity of **OS** (compensating for moisture as determined by duplicate TGA experiments) and sulfur totalling 10 g were weighed out and thoroughly mixed into a 20 mL scintillation vial equipped with a Teflon coated stir bar. The vials were sealed with rubber septa and flushed with N_2 for ten minutes. The vials were placed in an oil bath set to 180 °C. Samples were heated for $\sim$9 hours, frequently stopping the reaction by cooling to room temperature under N_2, manually scraping down the sides to help reincorporate the organic material, flushing for ten minutes with N_2, and placing back in the oil bath until homogenized. **OSS$_{90}$** was prepared first and then the procedures were replicated for **OSS$_{95}$** to ensure identical heating procedures. Specific heating times can be found in the ESI.†

Conflicts of interest

There are no conflicts to declare.

Acknowledgements

Notes and references

1 W. J. Chuang, J. J. Griebel, E. T. Kim, H. Yoon, A. G. Simmonds, H. J. Ji, P. T. Dirlam, R. S. Glass, J. J. Wie, N. A. Nguyen, B. W. Guralnick, J. Park, A. Somogyi, P. Theato, M. E. Mackay, Y.-E. Sung, K. Char and J. Pyun, *Nat. Chem.*, 2013, **5**, 518–524.

2 W. J. Chung, J. J. Griebel, E. T. Kim, A. G. Shimmonds, H.-S. Kim, R. S. Glass, Y.-E. Sung, K. Char and J. Pyun, *PMSE Preprints*, 2012.

3 M. K. Lauer, T. A. Estrada-Mendoza, C. D. McMillen, G. Chumanov, A. G. Tennyson and R. C. Smith, *Adv. Sustainable Syst.*, 2019, **3**, 1900062.

4 C. V. Lopez, C. P. Maladeniya and R. C. Smith, *Electrochem*, 2020, **1**, 226–259.

5 J. H. Worthington Max, L. Kucera Renata, T. Gibson Christopher, A. Sibley, D. Slattery Ashley, A. Campbell Jonathan, F. K. Alboaiji Salah, J. Young, N. Adamson, R. Gascooke Jason, A. Lewis David, S. Quinton Jamie, V. Ellis Amanda, M. Chalker Justin, S. Albuquerque Ines, J. L. Bernardes Goncalo, A. Muller Katherine, A. Johs, D. Jampaiah, M. Sabri Ylias, K. Bhargava Suresh and J. Ippolito Samuel, *Chemistry*, 2017, **23**, 16219–16230.

6 L. J. Esdaile and J. M. Chalker, *Chemistry*, 2018, **24**, 6905–6916.

7 M. J. H. Worthington, C. J. Shearer, L. J. Esdaile, J. A. Campbell, C. T. Gibson, S. K. Legg, Y. Yin, N. A. Lundquist, J. R. Gascooke, I. S. Albuquerque, J. G. Shapter, G. G. Andersson, D. A. Lewis, G. J. L. Bernardes and J. M. Chalker, *Adv. Sustainable Syst.*, 2018, **2**, 1800024.

8 Y. Zhang, T. S. Kleine, K. J. Carothers, D. D. Phan, R. S. Glass, M. E. MacKay, K. Char and J. Pyun, *Polym. Chem.*, 2018, **9**, 2290–2294.

9 Y. Zhang, J. J. Griebel, P. T. Dirlam, N. A. Nguyen, R. S. Glass, M. E. MacKay, K. Char and J. Pyun, *J. Polym. Sci., Part A: Polym. Chem.*, 2017, **55**, 107–116.

10 P. T. Dirlam, R. S. Glass, K. Char and J. Pyun, *J. Polym. Sci., Part A: Polym. Chem.*, 2017, **55**, 1635–1668.

11 T. S. Kleine, N. A. Nguyen, L. E. Anderson, S. Namnabat, E. A. LaVilla, S. A. Showghi, P. T. Dirlam, C. B. Arrington, M. S. Manchester, J. Schwiegerling, R. S. Glass, K. Char, R. A. Norwood, M. E. Mackay and J. Pyun, *ACS Macro Lett.*, 2016, **5**, 1152–1156.

12 P. T. Dirlam, A. G. Simmonds, T. S. Kleine, N. A. Nguyen, L. E. Anderson, A. O. Klever, A. Florian, P. J. Costanzo, P. Theato, M. E. Mackay, R. S. Glass, K. Char and J. Pyun, *RSC Adv.*, 2015, **5**, 24718–24722.

13 J. J. Griebel, G. Li, R. S. Glass, K. Char and J. Pyun, *J. Polym. Sci., Part A: Polym. Chem.*, 2015, **53**, 173–177.

14 J. J. Griebel, N. A. Nguyen, S. Namnabat, L. E. Anderson, R. S. Glass, R. A. Norwood, M. E. MacKay, K. Char and J. Pyun, *ACS Macro Lett.*, 2015, **4**, 862–866.

15 V. P. Oleshko, J. Kim, J. L. Schaefer, S. D. Hudson, C. L. Soles, A. G. Simmonds, J. J. Griebel, R. S. Glass, K. Char and J. Pyun, *MRS Commun.*, 2015, **5**, 353–364.

16 J. J. Griebel, N. A. Nguyen, A. V. Astashkin, R. S. Glass, M. E. MacKay, K. Char and J. Pyun, *ACS Macro Lett.*, 2014, **3**, 1258–1261.

17 S. Namnabat, J. J. Gabriel, J. Pyun and R. A. Norwood, *Proc. SPIE*, 2014, **8983**, 89830D.

18 A. G. Simmonds, J. J. Griebel, J. Park, K. R. Kim, W. J. Chung, V. P. Oleshko, J. Kim, E. T. Kim, R. S. Glass, C. L. Soles, Y.-E. Sung, K. Char and J. Pyun, *ACS Macro Lett.*, 2014, **3**, 229–232.

19 M. Mann, E. Kruger Jessica, F. Andari, J. McErlean, R. Gascooke Jason, A. Smith Jessica, J. H. Worthington Max, C. C. McKinley Cheylan, A. Campbell Jonathan, A. Lewis David, T. Hasell, V. Perkins Michael and M. Chalker Justin, *Org. Biomol. Chem.*, 2019, **17**, 1929–1936.

20 T. Hasell, D. J. Parker, H. A. Jones, T. McAllister and S. M. Howdle, *Chem. Commun.*, 2016, **52**, 5383–5386.

21 M. K. Lauer, A. G. Tennyson and R. C. Smith, *ACS Appl. Polym. Mater.*, 2020, **2**, 3761–3765.

22 M. S. Karunarathna, M. K. Lauer and R. C. Smith, *J. Mater. Chem. A*, 2020, **8**, 20318–20322.

23 T. Thiounn and R. C. Smith, *J. Polym. Sci.*, 2020, **58**, 1347–1364.

24 T. Thiounn, M. S. Karunarathna, L. M. Slann, M. K. Lauer and R. C. Smith, *J. Polym. Sci.*, 2020, **58**, 1347–1364.

25 S. J. Tonkin, C. T. Gibson, J. A. Campbell, D. A. Lewis, A. Karton, T. Hasell and J. M. Chalker, *Chem. Sci.*, 2020, **11**, 5537–5546.

26 N. A. Lundquist, A. D. Tikoalu, M. J. H. Worthington, R. Shapter, S. J. Tonkin, F. Stojcevski, M. Mann, C. T. Gibson, J. R. Gascooke, A. Karton, L. C. Henderson, L. J. Esdaile and J. M. Chalker, *Chem. – Eur. J.*, 2020, **26**, 10035–10044.

27 T. Thiounn, M. K. Lauer, M. S. Bedford, R. C. Smith and A. G. Tennyson, *RSC Adv.*, 2018, **8**, 39074–39082.

28 B. Zhang, H. Gao, P. Yan, S. Petcher and T. Hasell, *Mater. Chem. Front.*, 2020, **4**, 669–675.

29 P. Yan, W. Zhao, B. Zhang, L. Jiang, S. Petcher, J. A. Smith, D. J. Parker, A. I. Cooper, J. Lei and T. Hasell, *Angew. Chem., Int. Ed.*, 2020, **59**, 13371–13378.

30 C. R. Westerman and C. L. Jenkins, *Macromolecules*, 2018, **51**, 7233–7238.

31 C. R. Westerman, P. M. Walker and C. L. Jenkins, *J. Visualized Exp.*, 2019, e59620.

32 T. Thiounn, M. K. Lauer, M. S. Karunarathna, A. G. Tennyson and R. C. Smith, *Sustainable Chem.*, 2020, **1**, 183–197.

33 M. S. Karunarathna, M. K. Lauer, A. G. Tennyson and R. C. Smith, *Polym. Chem.*, 2020, **11**, 1621–1628.

34 S. Park, D. Lee, H. Cho, J. Lim and K. Char, *ACS Macro Lett.*, 2019, **8**, 1670–1675.

35 M. S. Karunarathna, A. G. Tennyson and R. C. Smith, *J. Mater. Chem. A*, 2020, **8**, 548–553.

36 A. D. Smith, R. C. Smith and A. G. Tennyson, *Sustainable Chem. Pharm.*, 2020, **16**, 100249.

37 A. D. Smith, C. D. McMillin, R. C. Smith and A. G. Tennyson, *J. Polym. Sci.*, 2020, **58**, 438–445.

38 A. D. Smith, T. Thiounn, E. W. Lyles, E. K. Kibler, R. C. Smith and A. G. Tennyson, *J. Polym. Sci., Part A: Polym. Chem.*, 2019, **57**, 1704–1710.

39 A. D. Smith, R. C. Smith and A. G. Tennyson, *Sustainable Chem.*, 2020, **1**, 209–237.

40 M. K. Lauer, M. S. Karunarathna, A. G. Tennyson and R. C. Smith, *Mater. Adv.*, 2020, **1**, 590–594.

41 M. K. Lauer, M. S. Karunarathna, G. Tennyson Andrew and R. C. Smith, *Mater. Adv.*, 2020, **1**, 2271–2278.

42 C. V. Lopez, M. S. Karunarathna, M. K. Lauer, C. P. Maladeniya, T. Thiounn, E. D. Ackley and R. C. Smith, *J. Polym. Sci.*, 2020, **58**, 2259–2266.

43 C. P. Maladeniya, M. S. Karunarathna, M. K. Lauer, C. V. Lopez, T. Thiounn and R. C. Smith, *Mater. Adv.*, 2020, **1**, 1665–1674.

44 T. Thiounn, A. G. Tennyson and R. C. Smith, *RSC Adv.*, 2019, **9**, 31460–31465.

45 M. S. Karunarathna and R. C. Smith, *Sustainability*, 2020, **12**, 734–748.

46 M. S. Karunarathna, M. K. Lauer, T. Thiounn, R. C. Smith and A. G. Tennyson, *J. Mater. Chem. A*, 2019, **7**, 15683–15690.

47 M. K. Lauer and R. C. Smith, *Compr. Rev. Food Sci. Food Saf.*, 2020, 1–53, DOI: 10.1111/1541-4337.12627.

48 L. Dai, J. Zhang and F. Cheng, *Int. J. Biol. Macromol.*, 2019, **132**, 897–905.

49 P. Paronen and M. Juslin, *J. Pharm. Pharmacol.*, 1983, **35**, 627–635.

50 N. A. S. Service, 2020 Corn Production: United States, https://www.nass.usda.gov/Charts_and_Maps/Field_Crops/cornprod.php.

51 U. S. D. o. Agriculture, USDA Coexistence Fact Sheets: Corn, 2015.

52 S. B. C. f. F. Agriculture, Back to Grass: The Market Potential for U.S. Grassfed Beef, 2017.

53 J. B. Olayanju, Top Trends Driving Change in the Food Industry, 2019.

54 B. Zhang, Q. Huang, F.-x. Luo, X. Fu, H. Jiang and J.-l. Jane, *Carbohydr. Polym.*, 2011, **84**, 1276–1281.

55 A. Naseri, H. Shekarchizadeh and M. Kadivar, *J. Food Process. Preserv.*, 2019, **43**, 1–10.

56 F. Chang, X. He, X. Fu, Q. Huang and Y. Qiu, *Food Chem.*, 2014, **152**, 177–183.

57 Z.-Y. Yu, S.-W. Jiang, Z. Zheng, X.-M. Cao, Z.-G. Hou, J.-J. Xu, H.-L. Wang, S.-T. Jiang and L.-J. Pan, *Int. J. Biol. Macromol.*, 2019, **137**, 277–285.

58 M. K. Lauer, T. A. Estrada-Mendoza, C. D. McMillen, G. Chumanov, A. G. Tennyson and R. C. Smith, *Adv. Sustainable Syst.*, 2019, **3**, 1900062.

59 M. K. Lauer, A. G. Tennyson and R. C. Smith, *ACS Appl. Polym. Mater.*, 2020, **2**, 3761–3765.

60 A. Smith and W. B. Holmes, *J. Am. Chem. Soc.*, 1905, **27**, 979–1013.

61 K. Frost, D. Kaminski, G. Kirwan, E. Lascaris and R. Shanks, *Carbohydr. Polym.*, 2009, **78**, 543–548.